

---

# A Channel Coding Benchmark for Meta-Learning

---

**Rui Li**  
 Samsung AI Center  
 Cambridge, UK  
 rui.li@samsung.com

**Ondrej Bohdal**  
 School of Informatics  
 University of Edinburgh, UK  
 ondrej.bohdal@ed.ac.uk

**Rajesh Mishra**  
 UT Austin, US  
 rajeshkmishra@  
 austin.utexas.edu

**Hyeji Kim**  
 UT Austin, US  
 hyeji.kim@  
 austin.utexas.edu

**Da Li, Nicholas Lane**  
 Samsung AI Center, UK  
 {da.li1, nic.lane}  
 @samsung.com

**Timothy Hospedales**  
 Samsung AI Center and  
 University of Edinburgh, UK  
 t.hospedales@ed.ac.uk

## Abstract

Meta-learning provides a popular and effective family of methods for data-efficient learning of new tasks. However, several important issues in meta-learning have proven hard to study thus far. For example, performance degrades in real-world settings where meta-learners must learn from a wide and potentially multi-modal distribution of training tasks; and when distribution shift exists between meta-train and meta-test task distributions. These issues are typically hard to study since the shape of task distributions, and shift between them are not straightforward to measure or control in standard benchmarks. We propose the *channel coding* problem as a benchmark for meta-learning. Channel coding is an important practical application where task distributions naturally arise, and fast adaptation to new tasks is practically valuable. We use this benchmark to study several aspects of meta-learning, including the impact of task distribution breadth and shift, which can be controlled in the coding problem. Going forward, this benchmark provides a tool for the community to study the capabilities and limitations of meta-learning, and to drive research on practically robust and effective meta-learners.

## 1 Introduction

Meta-learning, or learning-to-learn, aims to provide data-efficient learning of new tasks by training improved learning algorithms using a distribution over tasks. The promise of such data efficient learning has long inspired research [30; 33], and recently grown into a thriving research area in which rapid progress is being made [6; 42; 7; 11]. While performance has improved steadily, particularly on standard image recognition benchmarks, several fundamental outstanding challenges have been identified [11]. Notably, state of the art meta-learners have been shown to suffer in realistic settings [40; 35] when required to generalize across a diverse rather than artificially narrow range of tasks – i.e. the task distribution is broad and multi-modal; and when there is distribution shift between the (meta)training and (meta)testing tasks. These conditions are almost inevitable in real-world applications where, for example, robots should generalize across the range of manipulation tasks of interest to humans [40], and image recognition systems should cover a realistically wide range of image types [35]. However, systematic study of these issues is hampered because conventional benchmarks do not provide a way to quantitatively measure or control the complexity or similarity of task distributions: Does an image recognition benchmark covering birds and airplanes provide a more or less complex task distribution to meta-learn than one covering flowers and vehicles? Is there greater task-shift if a robot trained to pick up objects must adapt to opening a drawer or throwing a ball? In this paper, we contribute to the future study of these issues by introducing a *channel*

coding meta-learning benchmark, which enables finer control and measurement of task-distribution complexity and shift for study.

Channel coding is a classic problem in communications theory of how to encode/decode data to be transmitted over a capacity limited noisy channel so as to maximize the fidelity of the received transmission. While there is extensive theory on optimal codes for analytically tractable (e.g., Gaussian) channels, recent work has shown that codecs obtained by deep learning provide clearly superior performance on more complex challenging channels [15; 14]. In this paper, we focus on learning the *decoder* for a fixed encoder<sup>1</sup>. Best deep channel coding however is achieved by training codecs tuned to the noise properties of a given channel. Thus, a highly practical meta-learning problem arises: Meta-learning a channel code learner on a distribution of training channels, which can rapidly adapt to the characteristics of a newly encountered channel. By way of example, the role of meta-learning is now to enable the codec of a user’s mobile wireless device to rapidly adapt its coding algorithm for best reception as she traverses different environments or switches on/off other sources of interference.

In this paper, we introduce channel coding problems [14; 15] as tasks to study the performance of meta-learners and define a new benchmark to complement existing ones [40; 35]. Our benchmark spans five channel families, including a real-world measurement channel based on software defined radio (SDR). We show how the channel coding problem uniquely leads to natural model-agnostic ways to measure the *breadth* of a task distribution, as well as the *shift* between two task distributions (Fig 1) – quantities that are not straightforward to measure in computer vision benchmarks. Building on these metrics, we use our benchmarks to answer the following questions, among others:

**Q1:** *How vulnerable are existing meta-learners to underfitting when trained on complex task distributions?* Existing studies [40; 37] have identified this as a challenge but have not been able to study it systematically without task complexity measures. **Q2:** *How robust are existing meta-learners to task-distribution shift between meta-train and meta-test task distributions?* This challenge has been widely observed in both robotics [40] and computer vision [35; 10] but has not been able to be measured without task-distribution distance measures. **Q3:** *Are channel coding meta-learners able to rely on the feature re-use shortcut, or must they learn to adapt?* Meta-learners aim to learn how to adapt to new tasks, but recent studies have shown that in many cases they can exploit a shortcut of general purpose feature learning without adaptation [28; 39]. **Q4:** *Are gradient-based or feed-forward meta-learners better?* This has been widely debated in computer vision and robotics with inconclusive results [35; 40]. Finally, **Q5:** *How much can meta-learning benefit transmission error-rate on a real radio channel?.*

## 2 Background

### 2.1 Channel Coding Background

Channel coding is a key element in a communication system. Its role is to introduce controlled redundancy so that the receiver can reliably and efficiently recover the message from a *corrupted* received signal. A typical channel coding system consists of an encoder and a decoder, as illustrated in Fig. 2. In this example a rate 1/2 channel encoder maps  $K$  message bits  $\mathbf{b} \in \{0, 1\}^K$  to a length- $2K$  transmitted signal  $\mathbf{c} \in \{-1, 1\}^{2K}$ . In a more general setting a rate  $1/r$  encoder maps  $\mathbf{b} \in \{0, 1\}^K$  to  $\mathbf{c} \in \{\pm 1\}^{rK}$ . The signal  $\mathbf{c}$  is then transmitted with the noise effect experienced by the signal in the communication medium described by conditional distribution  $p(\mathbf{y}|\mathbf{c})$ , and channel outputs a noisy signal  $\mathbf{y} \sim p(\mathbf{y}|\mathbf{c})$ ,  $\mathbf{y} \in \mathbb{R}^{2K}$ . A canonical example is Additive White Gaussian Noise (AWGN) channels, where  $\mathbf{y} = \mathbf{c} + \mathbf{z}$  for Gaussian  $\mathbf{z} \sim \mathcal{N}(0, \sigma^2 I)$ . The decoder in turn takes the noisy signal as input and estimates the original message, i.e.  $\hat{\mathbf{b}} = f_\theta(\mathbf{y}) \in \{0, 1\}^K$ . The reliability of

<sup>1</sup>This is the practically relevant setting as communication standards defining the encoding protocol are not easy to change, but decoders can be upgraded without changing the standard.

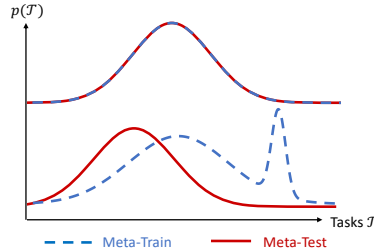


**Figure 1:** Schematic illustration of meta-learning scenarios. Top: The typical assumption of  $p_{tr}(\mathcal{T}) = p_{te}(\mathcal{T})$  is rarely met in practice. Bottom: (i) Given a complex distribution of training tasks, meta-learners may under-fit by failing to provide fast adaptation to all modes in the distribution. (ii): Realistic scenarios pose distribution shift between training  $p_{tr}(\mathcal{T})$  and deployment  $p_{te}(\mathcal{T})$ .

an encoder/decoder pair is measured by the probability of error, such as Bit Error Rate (BER) defined as  $\sum_{k=1}^K \mathbb{P}(\hat{b}_k \neq b_k)$ . We treat the decoding problem as a  $K$ -dimensional binary classification task for each of the ground-truth *message bits*  $b_k$ .

**Neural Decoder for Convolutional Codes** We focus on learning a decoder for a fixed rate 1/2 convolutional encoder which maps  $\mathbf{b} \in \{0, 1\}^K$  to  $\mathbf{c} \in \{\pm 1, 1\}^{2K}$  according to  $c_{2k} = 2(b_k + b_{k-1} + b_{k-2}) - 1$ ,  $c_{2k+1} = 2(b_k + b_{k-2}) - 1$  for  $k \in [1 : K]$  assuming  $b_0 = b_{-1} = 0$  (also illustrated in Appendix A). The sequential nature of convolutional encoding naturally aligns with convolutional neural networks. Practically, reliable and efficient decoders form an essential part of almost all kinds of communication systems, from wireline to wireless communications including both Wi-Fi and cellular. Thus there has been significant interest in applying deep learning to improve channel decoding (and coding itself) [25].

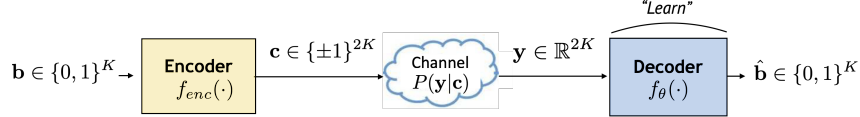


**Figure 2:** An illustration of the channel coding problem. We learn a channel decoder for a fixed encoder under various channel models.

**Adaptive Neural Decoder** The channel  $p(\mathbf{y}|\mathbf{c})$  can vary over time, and is unknown to the decoder. To help the decoder estimate the channel, pilot signals that are known messages  $\mathbf{b}_{known}$  are sent to the decoder before the transmission begins, so that the decoder can extract channel information from  $\mathbf{y}$  and  $\mathbf{b}_{known}$ . When modeling the decoder as a neural network instead of an analytical algorithm, one trains the decoder for a specific channel using pairs  $(\mathbf{y}, \mathbf{b}_{known})$  with pilot signals as ground-truths and their corresponding noisy received values as inputs. The optimization goal is to minimize a loss  $\mathcal{L}$ , which is typically in form of binary cross-entropy, with respect to decoder  $f_\theta$  as

$$\theta^* = \operatorname{argmin}_\theta \mathbb{E}_{\mathbf{b}_{known}, \mathbf{y}} \mathcal{L}(\mathbf{b}_{known}, f_\theta(\mathbf{y})) \quad (1)$$

To ensure good performance as channel characteristics  $p(\mathbf{y}|\mathbf{c})$  change due to e.g. weather or moving users, which always happen in realistic communications, the neural decoder  $f_\theta$  should adapt to evolving channel. Meta-learning is therefore a promising tool to enable rapid decoder adaptation with few pilot codes, as confirmed by early evidence [13]. Conversely, channel coding provides a lightweight benchmark for contemporary meta-learners, allowing control of the task complexity and distribution-shift, thanks to the mathematical representability and tractability of channel models.

**Connection to Standard Benchmarks** To clarify the connection to common vision benchmarks: Unique messages  $\mathbf{b}$  correspond to image categories, with noisy signals  $\mathbf{y}$  corresponding to individual images to recognize. The channel model  $p(\mathbf{y}|\mathbf{c}(\mathbf{b}))$  corresponds to the generative process for images conditional on a category; and our learned decoder  $f_\theta(\mathbf{y})$  corresponds to an image recognition model. Uniquely, we can control the generation process for data  $p(\mathbf{y}|\mathbf{c}(\mathbf{b}))$  which is not feasible for images.

## 2.2 Meta-Learning

Meta-learning usually considers distributions over tasks for training and testing  $p_{tr}(\mathcal{T})$  and  $p_{te}(\mathcal{T})$ . Each task  $\mathcal{T}_i$  is associated with a dataset  $D_i = \{\mathbf{x}_i^j, \mathbf{y}_i^j\}_{j=1}^J$ , which we split into  $D_i = D_i^{tr} \cup D_i^{val}$ . We are interested in learning models  $f_\theta$  of the form  $\hat{\mathbf{y}} = f_\theta(\mathbf{x})$  using some algorithm  $\mathcal{A}$  that minimizes a loss function  $\mathcal{L}(\theta, D)$  on data  $D$  with respect to parameters  $\theta$ . The algorithm itself is parameterized by meta-parameter  $\phi$ , i.e.,  $\theta^* = \mathcal{A}(D, \mathcal{L}, \phi)$ . The goal of meta-learning is to find the parameters  $\phi$  of algorithm  $\mathcal{A}$  that lead to strong validation performance after learning.

$$\phi^* = \operatorname{argmin} \mathbb{E}_{\substack{\mathcal{T} \sim p(\mathcal{T}) \\ (D^{tr}, D^{val}) \in \mathcal{T}}} \mathcal{L}(\mathcal{A}(D^{tr}, \mathcal{L}, \phi), D^{val}) \quad (2)$$

When datasets  $D^{tr}$  are small, this leads to meta-optimization for a data-efficient learner, as pioneered by MAML [6], which chooses meta-parameter  $\phi$  as the initial condition of the optimization for  $\theta$  by  $\mathcal{A}$ . Once meta-learning is complete, we can draw a new task  $\mathcal{T}' \sim p_{te}(\mathcal{T})$ , and solve it efficiently as

$$\theta^* = \mathcal{A}(D', \mathcal{L}, \phi^*). \quad (3)$$

### 3 Coding Benchmark for Meta-Learning

**Constructing Task Distributions** We consider five *families* of channel models and corresponding decoding tasks. These include synthetic Additive White Gaussian Noise (AWGN), Bursty, Memory noise, and Multipath interference channel used by 3GPP and ITU to decide which codecs to use in 4G LTE and 5G communication standards. Furthermore, we consider a final family consisting of data recorded from a real radio testbed (Software Defined Radios). See Appendix B for details. Each family is analogous to a dataset in common multi-dataset vision benchmarks [35]. All four synthetic channel families are used for meta-training, and the real wireless channel is held out for meta-testing.

To define task distributions, we consider uni-modal and multi-modal settings. In the *single-family, uni-modal* case, a task distribution  $p$  corresponds to a specific channel class as discussed above, parameterized by continuous channel parameters  $\omega$  (e.g., the variance of additive noise or multipath strength). The distribution of tasks in this family then depends on the prior over channel parameter  $\omega$ ,  $p(\mathcal{T}) = \int_{\omega} p(\mathcal{T}|\omega)p(\omega)$ . We can control the width of a task distribution by varying the width of the, e.g. uniform distributed, prior  $p(\omega)$ . In the *multi-family, multi-modal* case we can define a more complex task distribution as a mixture over multiple channel types  $p_k$ , each with its own distribution over channel parameters  $\omega$ ,  $p(\mathcal{T}) = \sum_k \int_{\omega} \pi_k p_k(\mathcal{T}|\omega)p_k(\omega)$ .

**Quantifying Task Distribution Shift and Breadth** We quantify the train-test task shift distance (Definition 1) and diversity of each task (Definition 2), based on information theoretic measures. In a coding benchmark, we can control these scores by choosing appropriate set of channel models, which allows us to evaluate the variability of meta-learning with the task distribution breadth and shift as illustrated in Fig 1. We demonstrate this in Section 4 (Fig. 4, 7).

**Definition 1 (Train-Test Task-Shift  $S(p_a(\mathcal{T}), p_b(\mathcal{T}))$ )** Simply *measuring* the shift between training and testing task distributions has previously been an open problem in meta-learning. However this becomes feasible to define for the channel coding problem. We quantify the distance between a test distribution  $p_a(\mathcal{T})$  and a training distribution  $p_b(\mathcal{T})$  using the Kullback–Leibler divergence (KLD) a.k.a. the relative entropy [18]. The KLD-based shift distance score is defined as:

$$S(p_a(\mathcal{T}), p_b(\mathcal{T})) := \mathbb{E}_{\mathbf{c}}[D_{KL}(p_a(\mathbf{y}_a|\mathbf{c})||p_b(\mathbf{y}_b|\mathbf{c}))] + \mathbb{E}_{\mathbf{c}}[D_{KL}(p_b(\mathbf{y}_b|\mathbf{c})||p_a(\mathbf{y}_a|\mathbf{c}))], \quad (4)$$

where  $p_a(\mathbf{y}_a|\mathbf{c})$  and  $p_b(\mathbf{y}_b|\mathbf{c})$  denote the channels associated with  $\mathcal{T}_a$  and  $\mathcal{T}_b$ , respectively. The distance is large if a testing distribution  $p_a$  introduces a very different distribution over received messages  $\mathbf{y}$  for a given code  $\mathbf{c}$  compared to training  $p_b$ , and zero if they induce the same distribution. One can also consider asymmetric KLD, i.e.,  $\mathbb{E}_{\mathbf{c}}[D_{KL}(p_a(\mathbf{y}_a|\mathbf{c})||p_b(\mathbf{y}_b|\mathbf{c}))]$  (See Appendix D).

**Definition 2 (Diversity Score  $D(\mathcal{T})$ )** The diversity score of a task distribution  $p(\mathcal{T})$  is defined as mutual information between the channel parameter  $\omega$  and the received signal  $\mathbf{y}$ :

$$D(\mathcal{T}) = \mathbb{E}_{\mathbf{c}}[I(\omega; \mathbf{y}|\mathbf{c})],$$

where  $\omega$  denotes the channel parameter (latent variable) for the task distribution, i.e.,  $p(\mathbf{y}|\mathbf{c}) = \int_{\omega} p(\mathbf{y}|\mathbf{c}, \omega)p_{\omega}(\omega)$ . We will see that this metric will quantify amenability to meta-learning. Intuitively, decoding benefits more from meta-learning when the channel distribution  $p(\mathbf{y}|\mathbf{c}, \omega)$  differs more across tasks (channel parameter  $\omega$ ). I.e., knowing the task conveys more information about  $\mathbf{y}$ .

**Estimation of Scores** In order to estimate shift-distance and diversity scores, we generate samples according to the corresponding task distributions and estimate each of these scores via Kraskov-Stögbauer-Grassberger (KSG) estimator [17; 32].

**Discussion** While we denote each channel to learn as a ‘*task*’, we note that in our application each task shares the same label-space of messages to recognize. As such our goal could also be understood as few-shot supervised adaptation to new *domains* by meta-learning. Thus our evaluation will compare to the simple domain generalization baseline of conventionally learning a decoder on all data from  $p_{tr}(\cdot)$  and applying it directly to tasks in  $p_{te}(\cdot)$  without adaptation.

### 4 Experiments

We first evaluate the impact of training distribution diversity on meta-learning performance, followed by that of train-test task distribution shift.

**Dataset and Task Design** We consider a wide range of channel scenarios that are described in Appendix C. To facilitate evaluation, we create a dataset of codewords and multiple transmitted messages under each channel model. For each of the benchmark scenarios, we created a dataset with 200 randomly sampled noise setups  $\omega$ , from the noise family specific to the scenario. Each noise setup has 50 randomly generated true codes (“classes”) with 50 examples (noisy received messages) for each type. When generating a meta-training task, we randomly sample a noise set-up and then randomly sample  $N$  codes with  $K$  support examples and  $L$  target or query examples. This makes the tasks similar to the standard  $N$ -way  $K$ -shot problems, but instead of a class-adaptation problem, we solve a fast domain-adaptation problem. For meta-testing, we have another dataset with 50 manually specified noise setups. For each noise setup we randomly generate 50 messages and with 50 examples each. The meta-testing dataset is shared across various scenarios. Meta-testing tasks are generated in the same way as meta-training tasks. All of the datasets are small enough to easily fit into the GPU memory, allowing fast experimentation.

**Meta-Learning Algorithms** We have evaluated a variety of meta-learning approaches. These include gradient-based learners **MAML** [6], its first order approximation **MAML FO**, **Reptile** [23], **ANIL** [28], **MetaSGD** [21], **KFO** [3], **MetaCurvature** [26] **CAVIA** [42] **BOIL** [24]; and feed-forward learners **ProtoNets** [31], **MetaBaseline** [5], and **FEAT** [38]. A description of these can be found in Appendix E. These are compared to the standard non-meta-learning approach of **empirical minimization (ERM)**, which trains a conventional neural decoder on the union of meta-training tasks, and has been shown to be a strong baseline [19; 9]. We have extended the implementations provided by *learn2learn* library [2] under the MIT License. Note that channel decoding is a *multi-label* problem that requires predicting a *vector* of bits for each input example, rather than a single multi-class classification. While this is straightforward for gradient-based meta-learners, we extended the implementation of the feed-forward meta-learners to support this.

**Hyperparameters and Architecture** All approaches used the same hyperparameters and CNN architecture for consistency. We used Adam optimizer with a meta-learning rate of 0.001 for the outer-loop, SGD with fine-tuning learning rate of 0.1 for the inner-loop consisting of 5 adaptation steps, 10 tasks in a meta-batch and 50000 meta-training iterations. Each task consisted of 5 different adaptation types (“classes”), with 5 support and 15 target examples. The ground truth messages are 10 bits long, encoded by the 1/2 rate convolutional encoder. Hence the message input to the decoder has shape  $1 \times 10 \times 2$ . We fix the decoder architecture as a CNN with 4 layers, 64 filters, kernel size 3, and stride 2. The CNN is followed by a linear fully-connected layer of size  $64 \times 10$ .

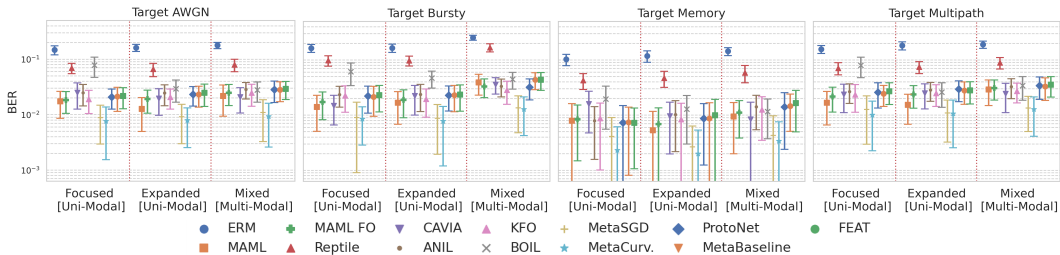


**Figure 3:** Meta-testing on AWGN, Bursty, Memory and Multipath task families (subplots). Y-axis is Bit Error Rate (BER, lower is better). Bars indicate meta-test standard-deviations. Left of the dashed line: Within-family setting compares uni-modal training distributions focused or widely distributed around the testing distribution. Right of the dashed line: Across-family setting where the training distribution is a mixture of all four task families including the testing distribution. Performance is only weakly impacted by diversity in the training distribution (compare focused→expanded→mixed).

#### 4.1 Impact of Training Distribution Diversity on Meta-Learning Performance

In this first section we investigate how meta-learners cope with task distributions of varying breadth and complexity, since previous studies have suggested that capacity could be a limiting factor of existing meta-learners [40; 29; 37]. We would like meta-learners to be capable of learning from a broad range of auxiliary tasks, without requiring the auxiliary task distribution to be carefully constructed in advance for similarity to each given target task (cf, Fig 1).

**Setup** In these experiments, we fix the meta-testing task distribution  $p_{te}(\mathcal{T})$  to ensure comparability, and then evaluate performance when the training distribution  $p_{tr}(\mathcal{T})$  is focused around the testing

condition ‘*focused*’ vs when it is spread more broadly around the testing distribution ‘*expanded*’. To expand the training distribution in the single-family/uni-modal case, we use a wider prior on the channel parameter  $p_{tr}^{expanded}(\omega) = \text{Unif}(a - \delta, b + \delta)$  vs  $p_{te}(\omega) = \text{Unif}(a, b)$  when constructing task distributions as discussed in Section 3. In the multi-modal case, we use a single channel family for  $p_{te}$  and a multi-modal mixture (‘*mixed*’) of families for  $p_{tr}$  composed of all the synthetic channel models (Appendix B) including the testing distribution  $p_{te}$ .

**Results** Fig. 3 summarizes the results for meta-learning on training distributions of varying widths for both uni-modal (marked as ‘*focused*’ and ‘*expanded*’) and multi-modal (marked as ‘*mixed*’) conditions, and for different target channels (four subplots). From the results, we can see that: (i) All meta-learners surpass the ERM baseline in every case, confirming the value of meta-learning based adaptation to channel type. (ii) Among the meta-learners, Reptile is worst; MetaSGD and MetaCurvature perform best indicating the value of learning not just initial condition but update direction and rate; and the others are in the middle. (iii) In the within-family case (left groups), focusing the meta-training distribution on the meta-testing condition (x-axis: *focused*) vs a diverse meta-training regime (x-axis: *expanded*) does not visibly affect meta-testing performance on our log-performance scale. In the across-family case (right, x-axis: *mixed*), transferring from a multi-modal training distribution to a specific testing distribution incurs a small but visible difference to performance. This suggests that while meta-learner capacity for fitting a multi-modal training distribution does impact performance [37; 29], it does so only in a minor way.

To further understand these results we compute the breadth of each training regime as measured by its *diversity* (Section 3). Note that we can measure the diversity of both *focused/expanded* (uni-modal) and *mixed* (multi-modal) training regimes with the same metric. As expected, the *mixed* regimes lead to higher diversity. Fig. 4 plots the margin between meta-learners and the vanilla non-adaptive baseline against the diversity score of the channel. We can see that, while more diverse training regimes slightly reduce absolute performance (Fig 3), the *benefit provided by meta-learning over vanilla ERM increases with more diverse training regimes* (Fig 4). Intuitively, the more the channel configuration parameters determine the output message distribution, the more potential benefit there is from meta-learning how to adapt to a given channel.

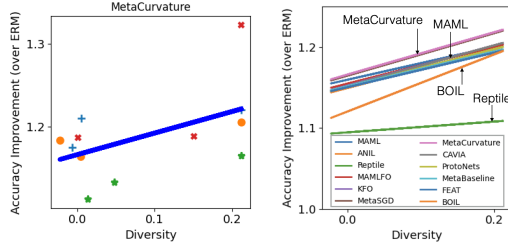


**Figure 4:** Correlation between task distribution diversity score and benefit of meta-learning. Left: Example fitting for MetaCurvature. X-axis: Diversity score of the channel; Y-axis: Accuracy gain over ERM. Symbols indicate different target channels from Fig 3 (o: AWGN, x: Bursty, \*: Memory, +: Multipath). Right: Fitted lines for all meta-learners. Learned adaptation strategies provide greater benefit on more diverse task distributions. Scatter plots for all meta-learners and the fitted curves are available in Appendix F.

## 4.2 Impact of Train-Test Distribution Shift on Meta-Learning Performance

**Within-Family Setup** We first illustrate the uni-modal within task family case, where we create distribution shift by setting  $p_{tr}(\omega) \neq p_{te}(\omega)$ . Specifically, we define two training task distributions using two different non-overlapping uniform priors on  $\omega$  corresponding to different channel SNRs (denoted ‘*high*’ and ‘*low*’) in the Bursty channel. We then train meta-learners on each, and evaluate them on a range of task parameters  $\omega$  that are both in- and out-of-domain with respect to the training distribution. In this section, we study how each of the baseline learners’ performance depends on distribution shift between training  $p_{tr}(\mathcal{T})$  and testing  $p_{te}(\mathcal{T})$  task distributions.

**Results** Fig. 5 shows the results of generalizing across a range of meta-testing tasks (x-axis), for models learned within each of the two specified training domains. Note that the ‘*difficulty*’ of the shown testing tasks is non-uniform i.e. higher SNR tasks are easier. This means that other things being equal we expect worse performance toward the left of the graphs; and that the models trained on the ‘*Low*’ SNR range (blue) and models trained on the ‘*High*’ SNR range (orange) have been exposed to the hardest/easiest training regime respectively. Concretely, the meta-learners’ performance is clearly better when operating within-domain than when operating with train-test distribution shift, indicated by the crossing of the lines corresponding to the two training conditions. Moreover, MetaCurvature appears to be stronger than MAML in both with and without task-shift conditions.

**Across-Family Setup** We next consider the more challenging across-family setting. In this case we create task distributions defined by each channel type and use them for meta-training. We then consider several channel types for meta-testing and evaluate pairs of matched and mis-matched train/test regimes. The four synthetic families are used for meta-training, and all five including our *real-world* channel dataset (See Appendix B for implementation details) are used for meta-testing. This setup aligns with the sim-to-real paradigm that is widely applied in other machine learning applications such as robotics and vision [34; 12] since it is easier to conduct large scale training on simulated data, and evaluate efficient-adaptation on sparser real-world data. We are the first to demonstrate and evaluate this meta-learning paradigm for channel coding applications.

**Results** From the results in Fig. 6, we can see that: (i) Meta-learning is generally most successful in the within-family condition; IE: when source channel on the x-axis matches the target channel of the sub-plot, as indicated by the dashed box. (ii) Some across-channel family conditions also perform quite well, such as Multipath  $\rightarrow$  AWGN; but not others, such as Bursty  $\rightarrow$  AWGN. (iii) However, some specific channel families such as Bursty cannot be successfully addressed when transferring from any other cross-family training distribution. (iv) The strongest methods MetaSGD and MetaCurvature perform consistently well in all setups.

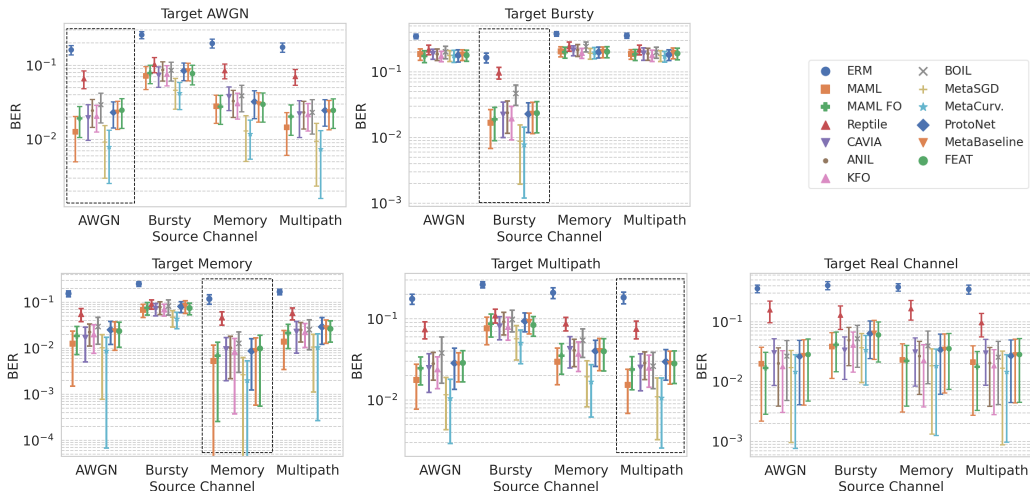


**Figure 6:** Impact of train-test distribution shift on decoding performance. Each sub-plot shows results of meta-testing on one of the AWGN, Bursty, Memory, Multipath task families, after learning on different meta-training channels (line groups, x-axis). Lines correspond to meta-test standard deviations of each algorithm. Boxes indicate when meta-training and meta-testing task families align, i.e., the within-family condition. Overall meta-learning works well within task distribution (boxes), and sometimes across task distribution.

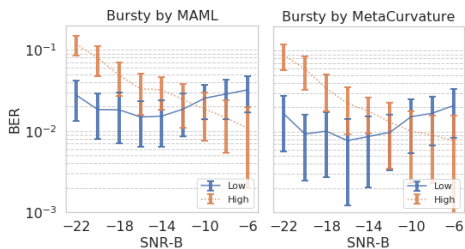


**Figure 5:** Impact of train-test distribution shift on decoding performance, within-family condition. X-axis: Meta-testing distribution parameter. Curves: Meta-training regime. “Low” training regime corresponds to lower SNR sampled from range (-2.5,3.5) and SNR-B from (-23, -17) for Bursty channel, and “High” training regime corresponds to SNR and SNR-B sampled from (8.5,13.5) and (-11, -5), respectively. Performance of meta-learners degrades relatively smoothly as decoders are evaluated in increasingly out-of-domain conditions (crossing high/low lines).

**Summary** We have seen in the previous two experiments that meta-learning performance is best when  $p_{te} = p_{tr}$ , with performance degrading smoothly when there is small deviation between them (Fig. 5), and sometimes dropping significantly when they are entirely different task families (Fig. 6). A key feature of channel coding as a meta-learning benchmark is the ability to measure the distance between task distributions in a systematic manner, as explained in Section 3. We can thus aggregate our results across experiments and plot normalized accuracy against meta-train meta-test task distribution distance as illustrated for MetaCurvature in Fig. 7 (left) (and in Appendix G). Here, each dot on the scatter plot is an experiment. In Fig. 7 (right) we fit compare the fitted performance curves for each meta-learner. We can see that they all have a positive relative accuracy slope: providing more benefit over vanilla ERM by adapting to in-

creasing train-test distribution shift. Going forward, the evaluation shown in Fig. 7 can provide a metric to benchmark the performance of meta-learners under train-test distribution shift. **Meta-Learned Decoders on a Real Wireless Channel** Notably, the results in Fig. 5 and Fig. 7 confirm that meta-learning is successful for the real wireless channel. The margins between the best and worst meta-learners when deployed on the real channel are somewhat smaller (Fig. 5(right)). However, the best meta-learners do provide 96% reduction in error rate compared to the standard neural decoder (ERM). This shows the potential of meta-learning for improving the performance of future real-world comms systems. It also shows benchmark’s value, as advancements in meta-learning driven by the benchmark can translate directly to real-world impact.

### 4.3 Comparison of Meta-Learners and Feature Reuse

**Comparison of Meta-Learners** Given the experiments so far, we can answer the question of which meta-learners are best (and worst) for adaptive channel coding. Aggregating across all the previous experiments, we report the *average rank* of each competitor in Figure 8(right). We conclude that: (i) MetaSGD and MetaCurvature provide the best performance. (ii) Reptile, BOIL and ANIL are the weakest. (iii) Comparing gradient-based and feed-forward meta-learners as a whole, the feed-forward methods never provide strong performance all with average rank below 6. Taken together these results suggest that feature adaptation (not performed by feed-forward models or ANIL), and in particular meta-learning how quickly to adapt each feature (MetaSGD and MetaCurvature) are crucial for high-performance adaptive coding.

**Feature Reuse** In computer vision, there has recently been a debate about whether meta-learning works for unexpected (feature-reuse) reasons [28; 39; 8], rather than the expected (fast-adaptation) reasons. In contrast, our coding benchmark results show that: Feature-reuse is not helpful (ANIL, which relies on feature-reuse, performs near-worst); and meta-learners rely on actual adaptation (learned learning rates are important for best performance). Thus coding appears less susceptible to feature re-use shortcuts observed in vision, and is a more reliable metric for meta-learning research.

To complement this claim, we make two further observations. First we note that for multi-domain learning, any *initial-condition* based meta-learner can be deployed in a zero-shot manner to meta-test tasks without adaptation. Fig. 8 (left) compares the performance of using each learner’s initialization directly with the performance after adaptation. We see that MetaSGD and MetaCurvature have some of the worst initializations, but the best performance after adaptation, confirming that they really do learn-to-adapt. Meanwhile Reptile provides the best initialization, but the worst performance post-adaptation. While disappointing as a meta-learner, this result is in line with [20] who observed that Reptile initialization provides a good baseline for robustness to domain-shift. Second, we employ Centered Kernel Alignment (CKA) [16] to evaluate how much each layer adapts to a task pre-and post few-shot adaptation and plot the results in Fig. 8 (middle) for MAML and MetaSGD for the list of experiments shown in Fig. 6. It can be observed that majority of the experiments require task adaptation of not only the classifier but also the feature layers. MetaSGD, which benefits from trainable adaption rates, updates both Conv. 1 & 2 more than MAML.

## 5 Discussion

**Summary** We presented a new meta-learning benchmark based on channel coding, a real-world and practically important problem that lends itself to meta-learning. We summarize by answering the questions we posed in the introduction. **Q1:** *How vulnerable are existing meta-learners to*

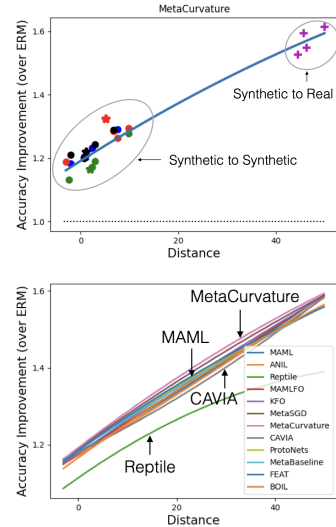


**Figure 7: Top:** Impact of train-test task distribution distance on decoding accuracy. X-axis: The KL distance score between train and test distributions (Eq. 4). Y-axis: accuracy gain over ERM. Left: Adaptive decoding with MetaCurvature. Each dot on the scatter plot corresponds to an experiment in Figure 3 (\*: shift from mixed channels) and Figure 6 (o: shift across-synthetic family), +: shift from synthetic channels to the real channel), where blue, red, green, black, and purple color corresponds to AWGN, Bursty, Memory, Multipath, and Real target channels, respectively. **Bottom:** Fitted curves for performance gain over ERM as a function of distance score. Scatter plots for all meta learners and the fitted curves are available in Appendix G.

under-fitting when trained on complex task distributions? Building on our task-distribution breadth metric, we quantified this relationship in (Fig 3,4). Our results show a relatively mild degradation in performance under complex task distributions compared to simple task distributions suggesting that this issue is not as severe as in robotics, for example [40]. Furthermore compared to zero-shot transfer of vanilla ERM, the benefit provided by meta-learning increases with distribution complexity. **Q2:** *How robust are existing meta-learners to task-distribution shift between meta-train and meta-test task distributions?* While absolute performance does decrease under distribution shift (Fig 6), by comparing our task distribution shift metric with relative improvement over ERM in Fig 7, we showed that performance *margin* of adaptive neural decoders actually tends to improve with distribution-shift. **Q3:** *Are channel coding meta-learners able to rely on the feature re-use shortcut, or must they learn to adapt?* Our analysis in Sec 4.3 showed that the feature re-use shortcut is not helpful for our coding benchmark, and meta-learners performance is indeed dominated by their learned ability to adapt. This reduced shortcut vulnerability suggests that our coding benchmark can play an important role in future meta-learner evaluation. **Q4:** *Are gradient-based or feed-forward meta-learners better?* While this question has been inconclusive in computer vision and robotics [35; 40], our results show that the recent gradient-based learners are clearly better than corresponding feed-forward meta-learners. This is presumably because feature adaptation is indeed crucial for channel-adaptive coding, and the feed-forward learners do not benefit from this. **Q5:** *How much can meta-learning benefit transmission error-rate on a real radio channel?* Our results show that a few pilot codes are sufficient for a meta-learned adaptive decoder to provide a substantial 96% reduction in error rate compared to a standard neural decoder. This confirms the practical value of this benchmark, as advances can translate to substantial improvements in comms performance.

**Application of Our Metrics to Conventional Tasks** A key contribution was a distance measure to quantify train-test task distribution shift. Our metric is in principle applicable to image classification, when two different task distributions share the label space such as in multi-domain learning [27]. However from practical perspective, estimating our metric for vision tasks is challenging because it would require an estimation of KL divergence between two distributions in high dimensional space (same as the dimension of the image). Similarly, our diversity measure also requires computing mutual information between input image (and the task distribution). One way to resolve this challenge is to measure our metric on low dimensional image representations and is left as future work.

**Future Work** In our evaluation, we considered a single instance of adaptation to new tasks, however in real applications with moving users the channel becomes a continuously varying environment. Thus coding could also serve as a systematic benchmark for continuous meta-learning [1], which has thus far suffered from lack of a simple and standardized benchmark. Meta-learning specifically in support of direct cross-domain robustness is also a topical branch of meta-learning [4], and such methods can be mapped directly onto our benchmark for evaluation as improvements to the ERM baseline in the case where no adaptation is allowed on target channels.

**Conclusion** Overall our benchmark has the advantage of elasticity in terms of number of tasks, instances, categories, difficulty of tasks, width of task distributions and train-test distribution shift. These properties make it suitable for purposes from fast prototyping to investigating the peak scalability of meta-learners, as well as issues in generalization and meta over/under-fitting. We hope the community will find it helpful for studying meta-learning going forward.

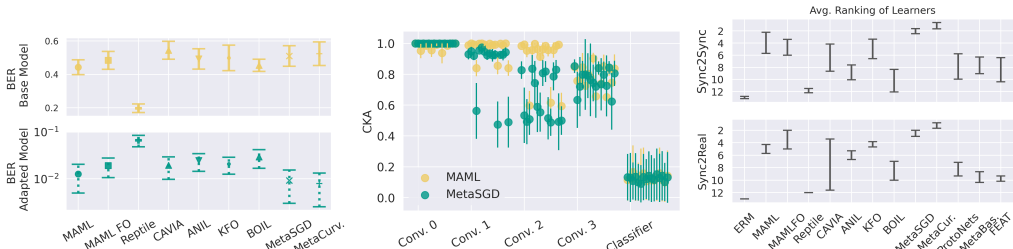


**Figure 8:** **Left:** Performance comparisons between base models, i.e. meta-learned initiations, and the adapted model. MetaCurvature and MetaSGD adapted models achieve low final BERs but the corresponding base models are associated with relatively higher BER, showing that they rely on a significant degree of fast adaptation. **Middle:** CKA-based similarity between model representations before and after adaptations across all experiments shown in Fig 6 for MAML and MetaSGD. All experiments do rely on feature adaptation and rather than head-only adaptation/feature reuse. MetaSGD learns to adapt the feature layers more than MAML. **Right:** Overall comparison of meta-learners in terms of average rank across all sync2sync and sync2real experiments.

## References

- [1] Maruan Al-Shedivat, Trapit Bansal, Yuri Burda, Ilya Sutskever, Igor Mordatch, and Pieter Abbeel. Continuous adaptation via meta-learning in nonstationary and competitive environments. In *ICLR*, 2018.
- [2] Sébastien M R Arnold, Praateek Mahajan, Debajyoti Datta, Ian Bunner, and Konstantinos Saitas Zarkias. learn2learn: A library for meta-learning research. In *arXiv*, 2020.
- [3] Sébastien M.R. Arnold, Shariq Iqbal, and Fei Sha. When MAML can adapt fast and how to assist when it cannot. In *AISTATS*, 2021.
- [4] Yogesh Balaji, Swami Sankaranarayanan, and Rama Chellappa. Metareg: Towards domain generalization using meta-regularization. In *NIPS*, 2018.
- [5] Yinbo Chen, Xiaolong Wang, Zhuang Liu, Huijuan Xu, and Trevor Darrell. A new meta-baseline for few-shot learning. *arXiv preprint arXiv:2003.04390*, 2020.
- [6] Chelsea Finn, Pieter Abbeel, and Sergey Levine. Model-agnostic meta-learning for fast adaptation of deep networks. In *ICML*, 2017.
- [7] Sebastian Flennerhag, Andrei A. Rusu, Razvan Pascanu, Francesco Visin, Hujun Yin, and Raia Hadsell. Meta-learning with warped gradient descent. In *ICLR*, 2020.
- [8] Micah Goldblum, Steven Reich, Liam Fowl, Renkun Ni, Valeriia Cherepanova, and Tom Goldstein. Unraveling meta-learning: Understanding feature representations for few-shot tasks. In *ICML*, 2020.
- [9] Ishaan Gulrajani and David Lopez-Paz. In search of lost domain generalization. In *ICLR*, 2021.
- [10] Yunhui Guo, Noel C Codella, Leonid Karlinsky, James V Codella, John R Smith, Kate Saenko, Tajana Rosing, and Rogerio Feris. A broader study of cross-domain few-shot learning. In *ECCV*, 2020.
- [11] Timothy M Hospedales, Antreas Antoniou, Paul Micaelli, and Amos J. Storkey. Meta-learning in neural networks: A survey. *IEEE Transactions on Pattern Analysis and Machine Intelligence*, pages 1–1, 2021.
- [12] Stephen James, Paul Wohlhart, Mrinal Kalakrishnan, Dmitry Kalashnikov, Alex Irpan, Julian Ibarz, Sergey Levine, Raia Hadsell, and Konstantinos Bousmalis. Sim-to-real via sim-to-sim: Data-efficient robotic grasping via randomized-to-canonical adaptation networks. In *CVPR*, 2019.
- [13] Yihan Jiang, Hyeji Kim, Himanshu Asnani, and Sreeram Kannan. Mind: Model independent neural decoder. In *IEEE International Workshop on Signal Processing Advances in Wireless Communications (SPAWC)*, 2019.
- [14] Hyeji Kim, Yihan Jiang, Sreeram Kannan, Sewoong Oh, and Pramod Viswanath. Deepcode: Feedback codes via deep learning. In *NIPS*, 2018.
- [15] Hyeji Kim, Yihan Jiang, Ranvir Rana, Sreeram Kannan, Sewoong Oh, and Pramod Viswanath. Communication algorithms via deep learning. In *ICLR*, 2018.
- [16] Simon Kornblith, Mohammad Norouzi, Honglak Lee, and Geoffrey Hinton. Similarity of neural network representations revisited. In *ICML*, 2019.
- [17] Alexander Kraskov, Harald Stögbauer, and Peter Grassberger. Estimating mutual information. *Phys. Rev. E*, 69:066138, 2004.
- [18] Solomon Kullback and Richard A Leibler. On information and sufficiency. *The annals of mathematical statistics*, 22(1):79–86, 1951.
- [19] Da Li, Yongxin Yang, Yi-Zhe Song, and Timothy M. Hospedales. Deeper, broader and artier domain generalization. In *ICCV*, 2017.

- [20] Yiying Li, Yongxin Yang, Wei Zhou, and Timothy M. Hospedales. Feature-critic networks for heterogeneous domain generalization. In *ICML*, 2019.
- [21] Zhenguo Li, Fengwei Zhou, Fei Chen, and Hang Li. Meta-SGD: Learning to learn quickly for few-shot learning. In *arXiv*, 2017.
- [22] Cuong V. Nguyen, Tal Hassner, Matthias Seeger, and Cedric Archambeau. Leep: A new measure to evaluate transferability of learned representations. In *ICML*, 2020.
- [23] Alex Nichol, Joshua Achiam, and John Schulman. On first-order meta-learning algorithms. In *arXiv*, 2018.
- [24] Jaehoon Oh, Hyungjun Yoo, ChangHwan Kim, and Se-Young Yun. Boil: Towards representation change for few-shot learning. In *Proc. Int. Conf. Learn. Represent.(ICLR)*, 2021.
- [25] T. O’Shea and J. Hoydis. An introduction to deep learning for the physical layer. *IEEE Transactions on Cognitive Communications and Networking*, 2017.
- [26] Eunbyung Park and Junier B Oliva. Meta-curvature. In *NeurIPS*, 2019.
- [27] Xingchao Peng, Qinxun Bai, Xide Xia, Zijun Huang, Kate Saenko, and Bo Wang. Moment matching for multi-source domain adaptation. In *ICCV*, 2019.
- [28] Aniruddh Raghu, Maithra Raghu, Samy Bengio, and Oriol Vinyals. Rapid learning or feature reuse? Towards understanding the effectiveness of maml. In *ICLR*, 2020.
- [29] Andrei A. Rusu, Dushyant Rao, Jakub Sygnowski, Oriol Vinyals, Razvan Pascanu, Simon Osindero, and Raia Hadsell. Meta-learning with latent embedding optimization. In *ICLR*, 2019.
- [30] Juergen Schmidhuber, Jieyu Zhao, and MA Wiering. Simple principles of metalearning. *Technical report IDSIA*, 69:1–23, 1996.
- [31] Jake Snell, Kevin Swersky, and Richard S. Zemel. Prototypical networks for few-shot learning. In *NIPS*, 2017.
- [32] Greg Ver Steeg. Non-parametric entropy estimation toolbox (NPEET), Nov 2014.
- [33] Sebastian Thrun and Lorien Pratt, editors. *Learning to learn*. Kluwer Academic Publishers, 1998.
- [34] Josh Tobin, Rachel Fong, Alex Ray, Jonas Schneider, Wojciech Zaremba, and Pieter Abbeel. Domain randomization for transferring deep neural networks from simulation to the real world. In *IEEE/RSJ international conference on intelligent robots and systems (IROS)*, 2017.
- [35] Eleni Triantafillou, Tyler Zhu, Vincent Dumoulin, Pascal Lamblin, Utku Evci, Kelvin Xu, Ross Goroshin, Carles Gelada, Kevin Swersky, Pierre-Antoine Manzagol, and Hugo Larochelle. Meta-dataset: A dataset of datasets for learning to learn from few examples. In *ICLR*, 2020.
- [36] Hung-Yu Tseng, Yi-Wen Chen, Yi-Hsuan Tsai, Sifei Liu, Yen-Yu Lin, and Ming-Hsuan Yang. Regularizing meta-learning via gradient dropout. In *ACCV*, 2020.
- [37] Risto Vuorio, Shao-Hua Sun, Hexiang Hu, and Joseph J. Lim. Multimodal model-agnostic meta-learning via task-aware modulation. In *NeurIPS*, 2019.
- [38] Han-Jia Ye, Hexiang Hu, De-Chuan Zhan, and Fei Sha. Few-shot learning via embedding adaptation with set-to-set functions. In *CVPR*, 2020.
- [39] Mingzhang Yin, George Tucker, Mingyuan Zhou, Sergey Levine, and Chelsea Finn. Meta-learning without memorization. In *ICLR*, 2020.
- [40] Tianhe Yu, Deirdre Quillen, Zhanpeng He, Ryan Julian, Karol Hausman, Chelsea Finn, and Sergey Levine. Meta-world: A benchmark and evaluation for multi-task and meta reinforcement learning. In *CORL*, 2019.
- [41] Hongyi Zhang, Moustapha Cisse, Yann N. Dauphin, and David Lopez-Paz. mixup: Beyond empirical risk minimization. In *ICLR*, 2018.
- [42] Luisa M Zintgraf, Kyriacos Shiarlis, Vitaly Kurin, Katja Hofmann, and Shimon Whiteson. Fast context adaptation via meta-learning. In *ICML*, 2019.

## Appendix

### A A Rate 1/2 Convolutional Encoder

A rate 1/2 convolutional code maps a length- $K$  message sequence to a length- $2K$  codeword in a sequential manner. At time  $k$ , the encoder is associated with a *state* represented by a two-dimensional binary vector  $s_k = (b_{k-1}, b_{k-2})$ . The encoder takes as input a binary variable  $b_k \in \{0, 1\}$  and generates a two-dimensional binary vector based on  $b_k$  and the state  $s_k$ . In particular, the codewords are generated according to  $c_{2k} = 2(b_k + b_{k-1} + b_{k-2}) - 1$ ,  $c_{2k+1} = 2(b_k + b_{k-2}) - 1$  for  $k \in [1 : K]$  assuming  $b_0 = b_{-1} = 0$ .

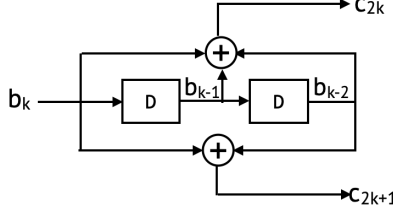


**Figure 9:** A rate 1/2 convolutional encoder considered throughout the paper

### B Channel Definitions

- AWGN( $\sigma^2$ ): Additive White Gaussian Noise (AWGN) channel is one of the most canonical channel model for communications, where i.i.d. Gaussian noise is added to the transmitted codeword, i.e.,  $\mathbf{y} = \mathbf{c} + \mathbf{z}$ , where  $\mathbf{z} \sim \mathcal{N}(0, \sigma^2 I)$ .
- Bursty ( $\sigma^2, \sigma_b^2, \alpha$ ): Bursty noise channel is a widely used channel model for interference or jamming scenarios, i.e.,  $\mathbf{y} = \mathbf{c} + \mathbf{z} + \mathbf{D}\mathbf{n}$ , where the background noise  $\mathbf{z} \sim \mathcal{N}(0, \sigma^2 I)$ , bursty noise  $\mathbf{n} \sim \mathcal{N}(0, \sigma_b^2 I)$  and  $\mathbf{D}$  is a diagonal matrix with  $D_{ii} \sim i.i.d. \text{Bern}(\alpha)$ .
- Memory Noise ( $\sigma^2, \alpha$ ): Noise with memory channels capture the scenario where noise at time  $i$  and noise at time  $j$  are correlated. Such channel is captured by the auto-regressive moving average (ARMA) of the noise, i.e.,  $\mathbf{y} = \mathbf{c} + \mathbf{z}$ , where  $z_i = \alpha z_{i-1} + \sqrt{1 - \alpha^2} n_i$ ,  $z_0 \sim \mathcal{N}(0, \sigma^2)$ ,  $\mathbf{n} \sim \mathcal{N}(0, \sigma^2 I)$ .
- Multipath ( $\sigma^2, \beta$ ): Multipath channel captures the effect of reflection in the communication medium, where the receiver receives the line-of-sight signal as well as multiple copies of the transmitted signal traversing different paths, and therefore associated with arbitrary delay and attenuation. We consider  $\mathbf{y} = \mathbf{c} + \beta \mathbf{c}^{\text{delayed}} + \mathbf{z}$ , where  $\mathbf{z} \sim \mathcal{N}(0, \sigma^2 I)$  and  $\mathbf{c}^{\text{delayed}}$  denotes  $\mathbf{c}$  delayed by a random delay  $d \sim \text{Unif}[1 : K]$ . Precisely,  $c_i^{\text{delayed}}$  is  $c_{i-d}$  if  $i > d$  and 0 otherwise.

#### Testbed Setup

The wireless testbed setup consists of two separate N200 USRPs operating as the transmitter and the receiver using antennas to communicate over air. The USRPs are connected to the system through the ethernet medium. We use MATLAB 2021 to preprocess and post-process the data while we use GNURadio to communicate with the USRPs. We derive the frame structure and the modulation parameters from the WiFi standard 802.11a. The transmit signals are arranged in frames with a preamble followed by data. The preamble consists of a short training sequence (STS) and a long training sequence (LTS). The encoded bits are mapped into 64-QAM symbols on the transmitter side and then modulated onto the subcarriers of the OFDM symbol along with the guard interval. The symbols also carry the pilot carriers in specific locations to aid in channel estimation and phase offset correction. These symbols are then converted to the time domain, appended by a cyclic prefix, and sent to the USRPs for transmission. Upon receiving the signal at the other USRP, we use the STS, and the LTS preambles for synchronization and frequency offset corrections. We remove the added cyclic prefix and convert the signal into frequency domain through an FFT. Lastly, we use the pilot

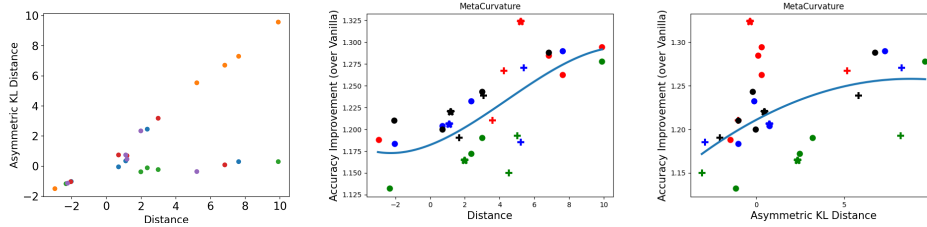


**Figure 10:** Left: Our distance vs. Asymmetric KL Divergence. Middle: Accuracy improvement vs. Distance for MetaCurvature. Right: Accuracy improvement vs. Symmetric KL Divergence. Each dot on the scatter plot is an experiment, and we fit lines for each model to show how MetaCurvature responds to increasingly different train-test task distributions.

carriers for channel equalization followed by demodulation to get the corresponding LLRs. The SNR of the transmission is managed by changing the transmit and receive power gains in order to achieve a requisite error performance mandated by the training procedure.

## C Experimental Details

We describe in this section the details of the experiment settings. Generally, instead of the statistic notion of  $\sigma$ , the notion of SNR is used by convention, specifically:  $\sigma = -20 * \log_{10} \text{SNR}$ . Similarly, for the Bursty channel,  $\sigma_b = -20 * \log_{10} \text{SNR}_b$ .

$$\sigma_b = -20 * \log_{10} \text{SNR}_b.$$

**Table 1:** Channel settings used in the study of train-test distribution shift in Fig. 5.

Parameter	SNR	SNR <sub>B</sub>
Low	[-2.5, 3.5]	[-23, -17]
High	[ 8.5, 13.5 ]	[ -11, -5]
Test	[ -22, -6]	[ -22, -6]

In the study of uni-modal training distributions **focused** or **expanded** as shown in Fig. 3, we sample channel parameters in the range shown in Table 2 for each specific setting. For the multi-modal setting, we combine the 4 channels using the “Expanded” range defined for each channel. The test setting is listed at the bottom row for each target type.

For the study of train-test distribution shift as shown in Fig. 5, we sample the channel parameters from the corresponding range, **Low** and **High**, as listed in Table 1. The trained model is tested in the range [-22, -6] with fixed step length 2.

Finally, in the across-family shift experiment in Fig. 6 models are trained and tested using data sampled from the “Expanded” range as described in Table. 2 and tested on the corresponding point of the target family, as shown in the last row of Table. 2.

**Table 2:** Channel parameter settings for the study of uni-modal training distributions **focused** or **expanded** around the testing distribution (Fig. 3) and the across-family distribution shift study shown in Fig. 6

Channel	AWGN	Bursty		Memory		Multipath	
Parameter	SNR	SNR	SNR <sub>B</sub>	SNR	$\alpha$	SNR	$\beta$
Focused	[-0.5, 0.5]	[5.5, 6.5]	[-15, -13]	[-0.5, 0.5]	[0.45, 0.55]	[-0.5, 0.5]	[0.45, 0.55]
Expanded	[-5, 5]	[1, 11]	[-19, -9]	[-5, 5]	[0.1, 0.9]	[-5, 5]	[0.1, 0.9]
Test	0	6	-14	0	0.5	0	0.5

## D Distance Metric

### Symmetric vs. asymmetric distance metric

There are several metrics to quantify the distance between two distributions. We use the KL distance. We take the average of the KL divergence between aaa and bbb. We empirically observe that the symmetrized KL divergence can be estimated more robustly. As shown in Figure 10 (left), the estimated asymmetric KL distance is close to zero for many scenarios where the distance between the training and test tasks are non-zero. Regardless of whether we measure the distance by the asymmetric KL divergence or by the symmetrized KL divergence, we observe that the improvement of meta-learners over vanilla increases as the distance increases (as shown in Figure 10 (middle, right)).

**Contrast with LEEP** There are a few measures proposed to quantify the distance between training and test tasks under various assumptions. [22] assumes that we have a model trained on one task and dataset for another task and introduce log expected empirical prediction (LEEP) metric, which quantifies how reliably the trained model can predict the label in the dataset.

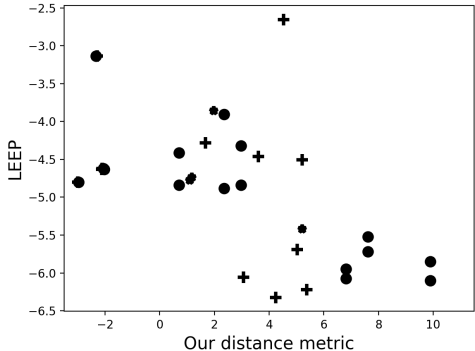


**Figure 11:** LEEP vs our distance metric. Each dot corresponds to a pair of training and test distributions. It can be seen that our distance metric and LEEP are highly correlated.

There are two key differences between our proposed distance metric and the LEEP metric. First, our metric is model agnostic and does not require training of any model. Second, our metric focuses on shift from a task *distribution* to another task *distribution* while LEEP focuses on shift from one deterministic task to another deterministic task. For our benchmark, we can evaluate LEEP score and compare the two metrics. We empirically show that our metric and LEEP are highly correlated as shown in Figure 11.

## E Meta-Learning Methods

In this paper, we have compared the following algorithms:

- **Vanilla** does not use meta-learning and directly trains a conventional model on the union of meta-training tasks. It is the empirical risk minimization *domain generalization* baseline for our benchmark, shown earlier to be a strong baseline [19; 9].
- **MAML** [6] is a meta-learner that aims to learn an initial condition for few-shot optimization by backpropagating through a few steps of gradient descent, exploiting higher-order gradients.
- **MAML FO** is the First-Order approximation to MAML introduced in [6], which saves computation by avoiding higher-order gradients.
- **Reptile** [23] is an efficient first-order alternative to MAML that moves the initial weights towards the weights obtained after fine-tuning on a task. It is also a strong baseline for domain generalization [20].
- **ANIL** (Almost No Inner Loop, [28]) is a simplification of MAML where only the task-specific network head (classifier) is included in the inner-loop updates. If ANIL performs similarly to MAML, it suggests that feature-reuse is the dominant factor, rather than rapid-tuning from the meta-learned initialization.

- **MetaSGD** [21] is an extended version of MAML where the meta-learner learns to update the direction as well as the learning rate for each parameter together with the initialization of the neural network.
- **KFO** (Meta Kronecker Factorized Optimizer, [3]) uses Kronecker factorization to transform the gradients and obtain more expressive and non-linear meta-optimizers. It improves on MAML on various computer vision benchmarks.
- **MetaCurvature** [26] builds on MAML and learns a curvature matrix together with initial parameters of the model. It outperforms MAML and MetaSGD in vision benchmarks.
- **CAVIA** [42] aims to reduce meta-overfitting in MAML by learning to adapt context parameters rather than the whole network. For CAVIA, we adopt the setting of employing 1 vector of 100 context parameters attaching to the 3<sup>rd</sup> layer of the network as in [42].
- **BOIL** (Body only inner loop [24]) is another effort to overcome feature reuse. BOIL only updates the feature layers in the inner loop while keeping the classifier frozen, inverting what ANIL proposes.
- **ProtoNets** [31] is one of the leading metric learning methods. Prototypical networks solve classification problem by building prototypes from support data and comparing query data against these prototypes based on Euclidean or cosine distances.
- **MetaBaseline** [5] builds upon ProtoNets and pre-trains a classifier on all base classes and then meta-learning on a nearest-centroid based few-shot classification algorithm.
- **FEAT** [38] leverages the relationship between target task instances and adapts the embedding for each task.

## F Accuracy vs. diversity for meta-learners

In Figure 13, we plot the accuracy improvement (over vanilla) as a function of the diversity for various meta-learners. We can see that for all meta-learners, the accuracy improvement increases as the diversity increases. In Figure 14, we show accuracy as a function of the diversity for various meta-learners. We can see that the absolute accuracy overall drops as the diversity score increases.

## G Accuracy vs. distance for meta-learners

In Figure 15, we plot the accuracy improvement (over vanilla) as a function of the train-test task distance for various meta-learners. As we can see from the figure, for all meta-learners, the accuracy improvement increases as the distance increases.

## H Additional Evaluation

### H.1 Impact of Number of Tasks on Meta-Learning Performance

Few studies have investigated how meta-learner performance depends on the number of meta-training tasks. This is partly because it is not straightforward in standard vision benchmarks to generate enough tasks (objects to recognize) to saturate performance with respect to task number. For our coding benchmark, we can sample an unlimited number of tasks (unique channels) to investigate this issue.

We consider both within- and across-family scenarios where models are trained on AWGN with expanded range ( $\text{SNR} \in [-5, 5]$ ), and tested on all 4 family types. For each learner we evaluate  $n \in \{200, 150, 100, 50, 40, 20\}$  unique tasks (domains/channel parameters) while keeping the total number of messages (categories to recognise), and total number of unique samples fixed.

Fig. 12 shows the BERs of each model as a function of the number of unique training channels, averaged over all four families of testing channels. Overall, most of the learners except for Reptile, which has relatively high BER in all settings, experience degradation in accuracy as the number of unique domains decreases. The ranking of absolute BER values remain constant as the number of domains changes, While the normalized BER curves suggest some meta-learners, e.g. ANIL, KFO, and MetaCurvature, experience more degradation in the sparse task regime than others e.g. CAVIA and MAML FO.

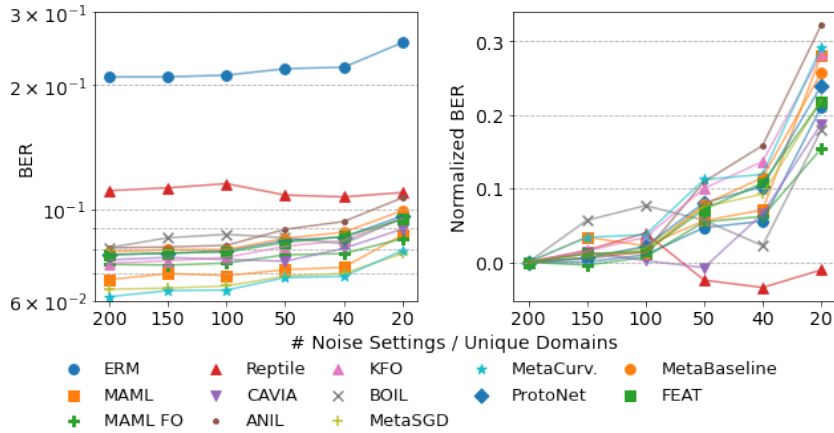


**Figure 12:** Dependence of error rate on number of unique domains (channel conditions). Left: Absolute values. Right: Normalized by BER of the corresponding learner when there are 200 domains.

## H.2 Evaluation of Meta-Augmentation

**Effectiveness of Meta-Augmentation** Task-level data augmentation is an emerging direction for improving meta-learner performance [39]. We evaluate the impact of the previously proposed DropGrad [36] and an adaptation of MixUp [41] to the few-shot meta-learning problem (see Appendix H.2 for details). We compute the average BER of the meta-learners using each augmentation strategy across our full suite of benchmarks. The results in Table 3 show our proposed adaptation of mixup consistently helps gradient-based meta-learners achieve better results, in contrast with the previous DropGrad. For metric-based learners, DropGrad is non-applicable, and MixUp does not improve the accuracy.

**Table 3:** Impact of meta-augmentation MixUp and DropGrad. Mean BER with its standard error across 17 different scenarios is reported.

LEARNER	MAML	ANIL	VANILLA	REPTILE	MAML FO	KFO
<b>BASELINE</b>	0.088 ± 0.007	0.093 ± 0.006	0.224 ± 0.006	0.115 ± 0.002	0.088 ± 0.007	0.086 ± 0.006
<b>MIXUP</b>	0.084 ± 0.005	0.085 ± 0.004	0.228 ± 0.007	0.105 ± 0.002	0.085 ± 0.005	0.085 ± 0.005
<b>DROPGRAD</b>	0.087 ± 0.006	0.093 ± 0.006	N/A	0.117 ± 0.001	0.088 ± 0.006	0.088 ± 0.006
METASGD	METACURVATURE	CAVIA	PROTONETS	METABASELINE	FEAT	BOIL
0.079 ± 0.006	0.074 ± 0.006	0.091 ± 0.007	0.090 ± 0.007	0.090 ± 0.006	0.088 ± 0.005	0.110 ± 0.009
0.074 ± 0.005	0.072 ± 0.005	0.091 ± 0.006	0.090 ± 0.006	0.090 ± 0.006	0.088 ± 0.005	0.102 ± 0.006
0.078 ± 0.006	0.074 ± 0.006	0.091 ± 0.007	N/A	N/A	N/A	0.110 ± 0.010

**Implementation Details** DropGrad randomly modifies the gradients within the inner-loop optimization, which has improved generalization to new few-shot learning tasks in the context of computer vision. We have chosen to use the Gaussian variant of DropGrad with rate  $p = 0.1$ , resulting in sampling noise terms  $n_g \sim N(1, \frac{0.1}{1-0.1})$ . This was a setting that worked well on computer vision few-shot learning reported in [36]. As DropGrad is only applicable to meta-learners that do fine-tuning, it is not applicable to vanilla as vanilla does not do any fine-tuning (hence value *N/A* in the table).

We adapt mixup in the following way:

1. Half of the tasks are clean and half are mixed.
2. When mixup is used, we randomly sample the number of “classes” (true messages) that will use it – at least one and at most all “classes” in the task.
3. Mixup rate  $\lambda$  is selected from  $U(0, 1)$  distribution and the same value is used consistently for all support and query examples of the given “class”.
4. When a “class” is mixed, we sample two original “classes” of the specified noise type to mix and use in the task.
5. Both encoded messages  $x_1, x_2$  and true messages  $y_1, y_2$  are interpolated to create a new message as  $x = \lambda x_1 + (1 - \lambda)x_2$  and  $y = \lambda y_1 + (1 - \lambda)y_2$ .

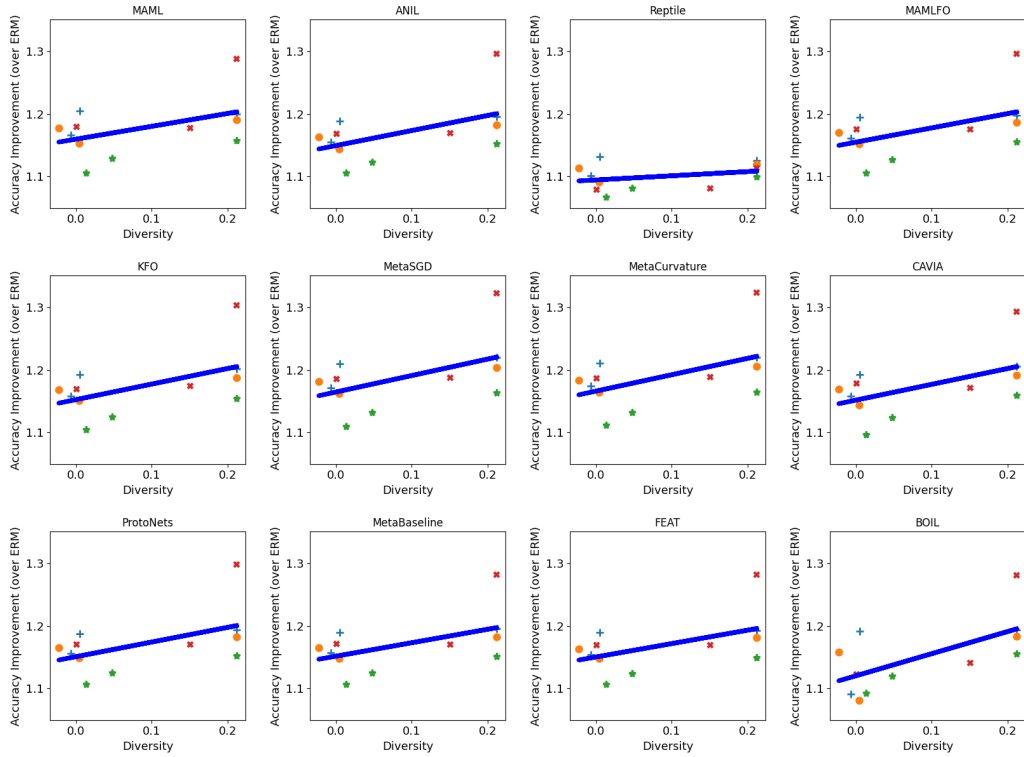


Figure 13: Accuracy improvement (over vanilla) vs. diversity for various meta-learners

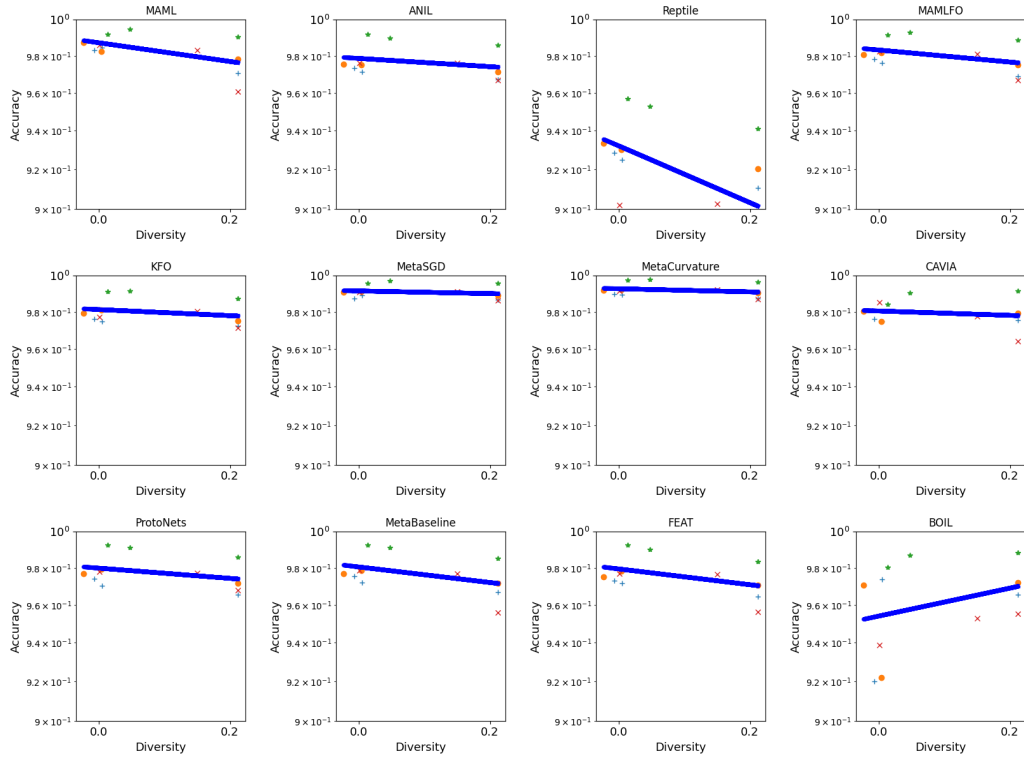
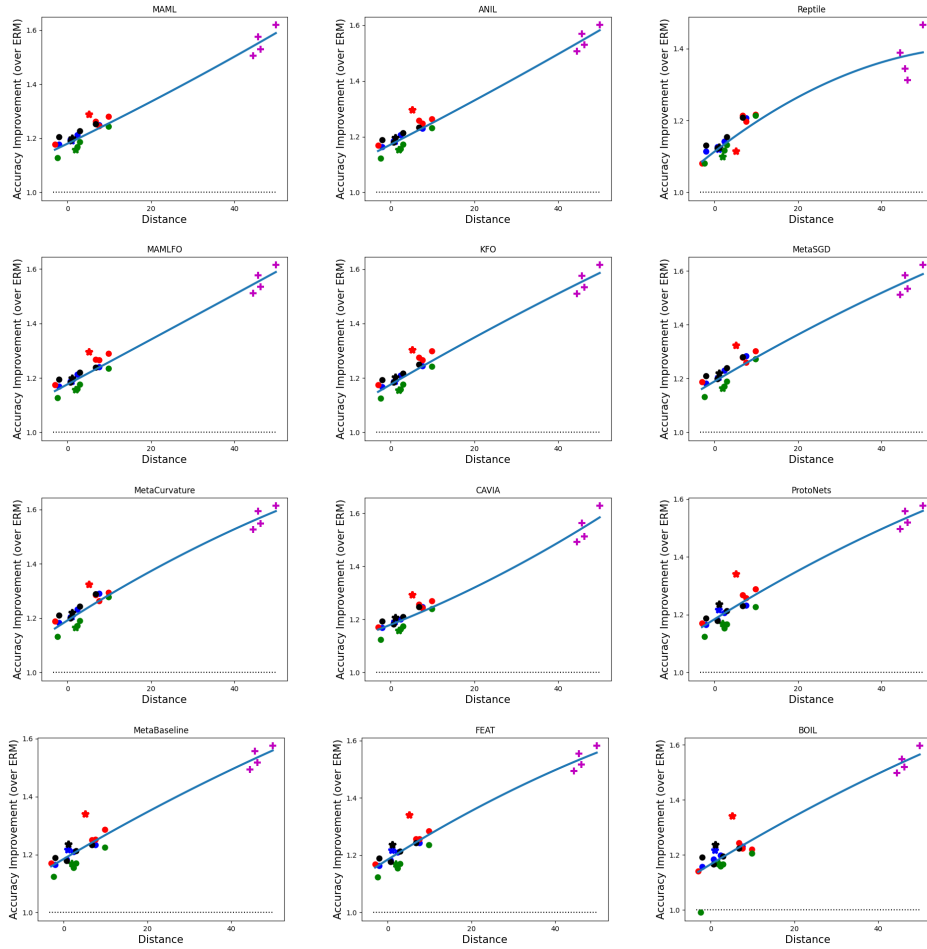


Figure 14: Accuracy vs. diversity for various meta-learners



**Figure 15:** Accuracy improvement (over ERM) vs. distance for various meta-learners